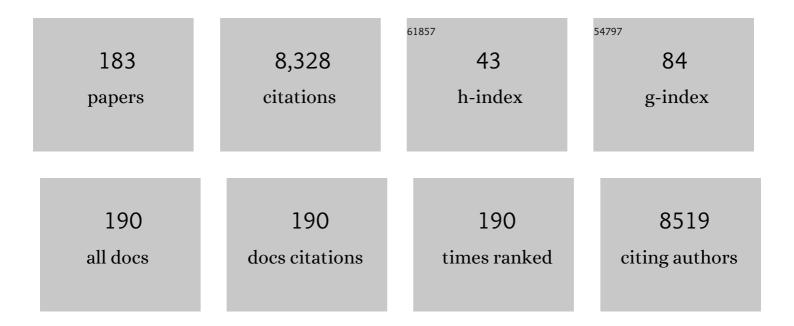
List of Publications by Year in descending order

Source: https://exaly.com/author-pdf/882499/publications.pdf Version: 2024-02-01



#	Article	IF	CITATIONS
1	Preparation of Silica Gel Obtained from Early Cretaceous Sidi Aich Sands (Central Tunisia) and its Potential to Remove Pollutant Dye Anionic from Wastwaters. Silicon, 2022, 14, 2351-2362.	1.8	3
2	Robocasting of 3D printed and sintered ceria scaffold structures with hierarchical porosity for solar thermochemical fuel production from the splitting of CO <sub>2</sub> . Nanoscale, 2022, 14, 4994-5001.	2.8	10
3	Unravelling the Affinity of Alkali-Activated Fly Ash Cubic Foams towards Heavy Metals Sorption. Materials, 2022, 15, 1453.	1.3	10
4	Cork derived TiO2 biomorphic ecoceramics. Open Ceramics, 2022, 9, 100243.	1.0	1
5	Green synthesis based X-type Ba–Zn Hexaferrites: Their structural, Hysteresis, Mӧssbauer, dielectric and electrical properties. Materials Chemistry and Physics, 2022, 282, 125914.	2.0	7
6	High colouring efficiency, optical density and inserted charge in sol–gel derived electrochromic titania nanostructures. Energy Advances, 2022, 1, 321-330.	1.4	3
7	Design and development of Ga-substituted Z-type hexaferrites for microwave absorber applications: Mössbauer, static and dynamic properties. Ceramics International, 2021, 47, 1145-1162.	2.3	29
8	Efficiency of natural clay and titania P25 composites in the decolouring of methylene blue (MB) from aqueous solutions: dual adsorption and photocatalytic processes. Arabian Journal of Geosciences, 2021, 14, 1.	0.6	8
9	Synthesis and characterisation of lead free BaFe12O19 –(K0.5Na0.5)NbO3 magnetoelectric composites, and the comparison of various synthetic routes. Journal of Alloys and Compounds, 2021, 883, 160819.	2.8	0
10	Pseudocapacitive behaviour in sol-gel derived electrochromic titania nanostructures. Nanotechnology, 2021, 32, 045703.	1.3	8
11	The role of calcium (source & content) on the in vitro behaviour of sol–gel quaternary glass series. Ceramics International, 2020, 46, 1065-1075.	2.3	4
12	Synthesis of red mud derived M-type barium hexaferrites with tuneable coercivity. Ceramics International, 2020, 46, 5757-5764.	2.3	3
13	Investigation of structural, magnetic and dielectric properties of gallium substituted Z-type Sr3Co2-Ga Fe24O41 hexaferrites for microwave absorbers. Journal of Alloys and Compounds, 2020, 822, 153470.	2.8	30
14	Biomimetic calcium carbonate with hierarchical porosity produced using cork as a sustainable template agent. Journal of Environmental Chemical Engineering, 2020, 8, 103594.	3.3	10
15	Geopolymer foams: An overview of recent advancements. Progress in Materials Science, 2020, 109, 100621.	16.0	161
16	Highly efficient lead extraction from aqueous solutions using inorganic polymer foams derived from biomass fly ash and metakaolin. Journal of Environmental Management, 2020, 272, 111049.	3.8	15
17	A Comparison of Bioactive Glass Scaffolds Fabricated ‎by Robocasting from Powders Made by Sol–Gel and Melt-Quenching Methods. Processes, 2020, 8, 615.	1.3	20
18	Solar Redox Cycling of Ceria Structures Based on Fiber Boards, Foams, and Biomimetic Cork-Derived Ecoceramics for Two-Step Thermochemical H <sub>2</sub> O and CO <sub>2</sub> Splitting. Energy & Fuels, 2020, 34, 9037-9049.	2.5	19

#	Article	IF	CITATIONS
19	Nanostructured titanium dioxide coatings prepared by Aerosol Assisted Chemical Vapour Deposition (AACVD). Journal of Photochemistry and Photobiology A: Chemistry, 2020, 400, 112727.	2.0	20
20	Studies of structural, magnetic and dielectric properties of X-type Barium Zinc hexaferrite Ba2Zn2Fe28O46 powder prepared by combustion treatment method using ginger root extract as a green reducing agent. Journal of Alloys and Compounds, 2020, 842, 155120.	2.8	28
21	High performance cork-templated ceria for solar thermochemical hydrogen production <i>via</i> two-step water-splitting cycles. Sustainable Energy and Fuels, 2020, 4, 3077-3089.	2.5	26
22	Films of chitosan and natural modified hydroxyapatite as effective UV-protecting, biocompatible and antibacterial wound dressings. International Journal of Biological Macromolecules, 2020, 159, 1177-1185.	3.6	32
23	Bonded ferrite-based exchange-coupled nanocomposite magnet produced by Warm compaction. Journal Physics D: Applied Physics, 2020, 53, 494003.	1.3	8
24	Robocasting: Prediction of ink printability in solgel bioactive glass. Journal of the American Ceramic Society, 2019, 102, 1608-1618.	1.9	13
25	Cytotoxicity and bioactivity assessments for Cu <sup>2+</sup> and La <sup>3+</sup> doped highâ€silica solâ€gel derived bioglasses: The complex interplay between additive ions revealed. Journal of Biomedical Materials Research - Part A, 2019, 107, 2680-2693.	2.1	7
26	Enhancement of maximum energy product in exchange-coupled BaFe12O19/Fe3O4 core-shell-like nanocomposites. Journal of Alloys and Compounds, 2019, 806, 120-126.	2.8	28
27	Octylamine as a novel fuel for the preparation of magnetic iron oxide particles by an aqueous auto–ignition method. Journal of Alloys and Compounds, 2019, 805, 545-550.	2.8	3
28	Pyrolysed cork-geopolymer composites: A novel and sustainable EMI shielding building material. Construction and Building Materials, 2019, 229, 116930.	3.2	28
29	A Review of Solar Thermochemical CO2 Splitting Using Ceria-Based Ceramics With Designed Morphologies and Microstructures. Frontiers in Chemistry, 2019, 7, 601.	1.8	72
30	Employment of phosphate solubilising bacteria on fish scales – Turning food waste into an available phosphorus source. Journal of Environmental Chemical Engineering, 2019, 7, 103403.	3.3	12
31	Clove and cinnamon: Novel anti–oxidant fuels for preparing magnetic iron oxide particles by the sol–gel auto–ignition method. Journal of Alloys and Compounds, 2019, 786, 71-76.	2.8	10
32	Guidelines to adjust particle size distributions by wet comminution of a bioactive glass determined by Taguchi and multivariate analysis. Ceramics International, 2019, 45, 3857-3863.	2.3	6
33	Comparison of low and high pressure infiltration regimes on the density and highly porous microstructure of ceria ecoceramics made from sustainable cork templates. Journal of the European Ceramic Society, 2019, 39, 1287-1296.	2.8	12
34	Robocasting of Cu2+ & La3+ doped sol–gel glass scaffolds with greatly enhanced mechanical properties: Compressive strength up to 14†MPa. Acta Biomaterialia, 2019, 87, 265-272.	4.1	18
35	In-depth investigation of the long-term strength and leaching behaviour of inorganic polymer mortars containing green liquor dregs. Journal of Cleaner Production, 2019, 220, 630-641.	4.6	12
36	A sustainable multi-function biomorphic material for pollution remediation or UV absorption: Aerosol assisted preparation of highly porous ZnO-based materials from cork templates. Journal of Environmental Chemical Engineering, 2019, 7, 102936.	3.3	19

#	Article	IF	CITATIONS
37	Red mud-based inorganic polymer spheres bulk-type adsorbents and pH regulators. Materials Today, 2019, 23, 105-106.	8.3	8
38	The effects of Cu2+ and La3+ doping on the sintering ability of sol-gel derived high silica bioglasses. Ceramics International, 2019, 45, 10269-10278.	2.3	6
39	Sustainable and efficient cork - inorganic polymer composites: An innovative and eco-friendly approach to produce ultra-lightweight and low thermal conductivity materials. Cement and Concrete Composites, 2019, 97, 107-117.	4.6	38
40	Robocasting of ceramic glass scaffolds: Sol–gel glass, new horizons. Journal of the European Ceramic Society, 2019, 39, 1625-1634.	2.8	28
41	Effect of surfactants on the optical and magnetic properties of cobalt-zinc ferrite Co0.5Zn0.5Fe2O4. Journal of Alloys and Compounds, 2019, 774, 1250-1259.	2.8	48
42	Synthesis of porous biomass fly ash-based geopolymer spheres for efficient removal of methylene blue from wastewaters. Journal of Cleaner Production, 2019, 207, 350-362.	4.6	140
43	Stress induced magnetic-domain evolution in magnetoelectric composites. Nanotechnology, 2018, 29, 255702.	1.3	4
44	The influence of processing parameters on morphology and granulometry of a wet-milled sol-gel glass powder. Ceramics International, 2018, 44, 12754-12762.	2.3	7
45	Effects of catalysts on polymerization and microstructure of solâ€gel derived bioglasses. Journal of the American Ceramic Society, 2018, 101, 2831-2839.	1.9	10
46	Influence of Mg substitution on structural, magnetic and dielectric properties of X-type barium zinc hexaferrites Ba2Zn2-xMgxFe28O46. Journal of Alloys and Compounds, 2018, 741, 377-391.	2.8	100
47	Enhanced bioactivity of a rapidly-dried sol-gel derived quaternary bioglass. Materials Science and Engineering C, 2018, 91, 36-43.	3.8	18
48	Structural and complex electromagnetic properties of cobalt ferrite (CoFe2O4) with an addition of niobium pentoxide. Ceramics International, 2018, 44, 915-921.	2.3	12
49	Synthesis and bioactivity assessment of high silica content quaternary glasses with <scp>C</scp> a: <scp>P</scp> ratios of 1.5 and 1.67, made by a rapid solâ€gel process. Journal of Biomedical Materials Research - Part A, 2018, 106, 510-520.	2.1	13
50	BIONANOSCULP, an ongoing project in biotechnology applications for preventive conservation of outdoor sculptures. IOP Conference Series: Materials Science and Engineering, 2018, 364, 012075.	0.3	0
51	One-Step Synthesis, Structure, and Band Gap Properties of SnO <sub>2</sub> Nanoparticles Made by a Low Temperature Nonaqueous Sol–Gel Technique. ACS Omega, 2018, 3, 13227-13238.	1.6	83
52	Biotechnology for Preventive Conservation: Development of Bionanomaterials for Antimicrobial Coating of Outdoor Sculptures. Studies in Conservation, 2018, 63, 230-233.	0.6	2
53	Solar thermochemical CO2 splitting using cork-templated ceria ecoceramics. Journal of CO2 Utilization, 2018, 26, 552-563.	3.3	42
54	Innovative application for bauxite residue: Red mud-based inorganic polymer spheres as pH regulators. Journal of Hazardous Materials, 2018, 358, 69-81.	6.5	56

#	Article	IF	CITATIONS
55	Extremely fast and efficient methylene blue adsorption using eco-friendly cork and paper waste-based activated carbon adsorbents. Journal of Cleaner Production, 2018, 197, 1137-1147.	4.6	106
56	A sustainable replacement for TiO2 in photocatalyst construction materials: Hydroxyapatite-based photocatalytic additives, made from the valorisation of food wastes of marine origin. Journal of Cleaner Production, 2018, 193, 115-127.	4.6	22
57	Incorporation of glass fibre fabrics waste into geopolymer matrices: An eco-friendly solution for off-cuts coming from wind turbine blade production. Construction and Building Materials, 2018, 187, 876-883.	3.2	38
58	Sequential piezoresponse force microscopy and the â€~small-data' problem. Npj Computational Materials, 2018, 4, .	3.5	14
59	Magnetic and Nanostructural Properties of Cobalt–Zinc Ferrite for Environmental Sensors. , 2018, , 1-18.		0
60	Ecoceramics. Materials Today, 2017, 20, 45-46.	8.3	18
61	Surface modified hydroxyapatites with various functionalized nanostructures: Computational studies of the vacancies in HAp. Ferroelectrics, 2017, 509, 105-112.	0.3	3
62	Purely Visible-Light-Induced Photochromism in Ag–TiO <sub>2</sub> Nanoheterostructures. Langmuir, 2017, 33, 4890-4902.	1.6	38
63	Production of silica gel from Tunisian sands and its adsorptive properties. Journal of African Earth Sciences, 2017, 130, 238-251.	0.9	16
64	A hundred times faster: Novel, rapid solâ€gel synthesis of bioâ€glass nanopowders (Siâ€Naâ€Caâ€P system, Ca:	P =) Tj ETC 1.0	QqQ 0 0 rgBT
65	Biphasic apatite-carbon materials derived from pyrolysed fish bones for effective adsorption of persistent pollutants and heavy metals. Journal of Environmental Chemical Engineering, 2017, 5, 4884-4894.	3.3	47
66	Effective mechanical reinforcement of inorganic polymers using glass fibre waste. Journal of Cleaner Production, 2017, 166, 343-349.	4.6	41
67	Photocatalytic nano-composite architectural lime mortar for degradation of urban pollutants under solar and visible (interior) light. Construction and Building Materials, 2017, 152, 206-213.	3.2	17
68	Aerosol assisted chemical vapour deposition of hydroxyapatite-embedded titanium dioxide composite thin films. Journal of Photochemistry and Photobiology A: Chemistry, 2017, 332, 45-53.	2.0	36
69	Effect of preparation and processing conditions on UV absorbing properties of hydroxyapatite-Fe2O3 sunscreen. Materials Science and Engineering C, 2017, 71, 141-149.	3.8	30
70	Novel route for rapid sol-gel synthesis of hydroxyapatite, avoiding ageing and using fast drying with a 50-fold to 200-fold reduction in process time. Materials Science and Engineering C, 2017, 70, 796-804.	3.8	59
71	Aqueous Acid Orange 7 dye removal by clay and red mud mixes. Applied Clay Science, 2016, 126, 197-206.	2.6	52
72	Oxygen vacancies, the optical band gap (Eg) and photocatalysis of hydroxyapatite: Comparing modelling with measured data. Applied Catalysis B: Environmental, 2016, 196, 100-107.	10.8	146

#	Article	IF	CITATIONS
73	Sensing properties and photochromism of Ag–TiO <sub>2</sub> nano-heterostructures. Journal of Materials Chemistry A, 2016, 4, 9600-9613.	5.2	45
74	Pt-decorated In2O3 nanoparticles and their ability as a highly sensitive (<10 ppb) acetone sensor for biomedical applications. Sensors and Actuators B: Chemical, 2016, 230, 697-705.	4.0	97
75	High dielectric constant and capacitance in ultrasmall (2.5 nm) SrHfO <sub>3</sub> perovskite nanoparticles produced in a low temperature non-aqueous sol–gel route. RSC Advances, 2016, 6, 51493-51502.	1.7	19
76	Biomimetic cork-based CeO2 ecoceramics for hydrogen generation using concentrated solar energy. Ciência & Tecnologia Dos Materiais, 2016, 28, 23-28.	0.5	6
77	Smallest Bimetallic CoPt <sub>3</sub> Superparamagnetic Nanoparticles. Journal of Physical Chemistry Letters, 2016, 7, 4039-4046.	2.1	12
78	Valorisation of industrial iron oxide waste to produce magnetic barium hexaferrite. ChemistrySelect, 2016, 1, 819-825.	0.7	5
79	Effective removal of anionic and cationic dyes by kaolinite and TiO <sub>2</sub> /kaolinite composites. Clay Minerals, 2016, 51, 19-27.	0.2	44
80	Effects of Cu, Zn and Cu-Zn addition on the microstructure and antibacterial and photocatalytic functional properties of Cu-Zn modified TiO 2 nano-heterostructures. Journal of Photochemistry and Photobiology A: Chemistry, 2016, 330, 44-54.	2.0	27
81	Fast route for synthesis of stoichiometric hydroxyapatite by employing the Taguchi method. Materials and Design, 2016, 109, 547-555.	3.3	20
82	The Influence of Cu <sup>2+</sup> and Mn <sup>2+</sup> Ions on the Structure and Crystallization of Diopside–Calcium Pyrophosphate Bioglasses. International Journal of Applied Glass Science, 2016, 7, 345-354.	1.0	5
83	The effect of functional ions (Y3+, Fâ~', Ti4+) on the structure, sintering and crystallization of diopside-calcium pyrophosphate bioglasses. Journal of Non-Crystalline Solids, 2016, 443, 162-171.	1.5	12
84	Combinatorial Materials Science, and a Perspective on Challenges in Data Acquisition, Analysis and Presentation. Springer Series in Materials Science, 2016, , 241-270.	0.4	2
85	Hidden value in low-cost inorganic pigments as potentially valuable magnetic materials. Ceramics International, 2016, 42, 9605-9612.	2.3	7
86	Truncated tetragonal bipyramidal anatase nanocrystals formed without use of capping agents from the supercritical drying of a TiO <sub>2</sub> sol. CrystEngComm, 2016, 18, 164-176.	1.3	13
87	Influence of sol counter-ions on the anatase-to-rutile phase transformation and microstructure of nanocrystalline TiO <sub>2</sub> . CrystEngComm, 2015, 17, 1813-1825.	1.3	11
88	Local manifestations of a static magnetoelectric effect in nanostructured BaTiO <sub>3</sub> –BaFe <sub>12</sub> O <sub>9</sub> composite multiferroics. Nanoscale, 2015, 7, 4489-4496.	2.8	32
89	Nitrogen-modified nano-titania: True phase composition, microstructure and visible-light induced photocatalytic NO abatement. Journal of Solid State Chemistry, 2015, 231, 87-100.	1.4	18
90	Hydroxyapatite-based materials of marine origin: A bioactivity and sintering study. Materials Science and Engineering C, 2015, 51, 309-315.	3.8	53

#	Article	IF	CITATIONS
91	Nano-titania doped with europium and neodymium showing simultaneous photoluminescent and photocatalytic behaviour. Journal of Materials Chemistry C, 2015, 3, 4970-4986.	2.7	45
92	Silver-containing calcium phosphate materials of marine origin with antibacterial activity. Ceramics International, 2015, 41, 10152-10159.	2.3	24
93	Magnetic wood-based biomorphic Sr3Co2Fe24O41 Z-type hexaferrite ecoceramics made from cork templates. Materials and Design, 2015, 82, 297-303.	3.3	24
94	Computational study of hydroxyapatite structures, properties and defects. Journal Physics D: Applied Physics, 2015, 48, 195302.	1.3	59
95	Cu–TiO <sub>2</sub> Hybrid Nanoparticles Exhibiting Tunable Photochromic Behavior. Journal of Physical Chemistry C, 2015, 119, 23658-23668.	1.5	37
96	Quantitative XRD characterisation and gas-phase photocatalytic activity testing for visible-light (indoor applications) of KRONOClean 7000®. RSC Advances, 2015, 5, 102911-102918.	1.7	40
97	Novel nanosynthesis of In <sub>2</sub> O <sub>3</sub> and its application as a resistive gas sensor for sevoflurane anesthetic. Journal of Materials Chemistry B, 2015, 3, 399-407.	2.9	21
98	Light induced antibacterial activity and photocatalytic properties of Ag/Ag3PO4 -based material of marine origin. Journal of Photochemistry and Photobiology A: Chemistry, 2015, 296, 40-47.	2.0	50
99	Characterization and antimicrobial properties of food packaging methylcellulose films containing stem extract of Ginja cherry. Journal of the Science of Food and Agriculture, 2014, 94, 2097-2103.	1.7	21
100	Magnetic Properties of Aligned <scp>C</scp> o <sub>2</sub> <scp>Z</scp> Hexagonal <scp>Z</scp> â€Ferrite Fibers. International Journal of Applied Ceramic Technology, 2014, 11, 451-456.	1.1	5
101	Magnetic Properties of Ferrite Ceramics Made from Wastes. Waste and Biomass Valorization, 2014, 5, 133-138.	1.8	12
102	Hydroxyapatite and chloroapatite derived from sardine by-products. Ceramics International, 2014, 40, 13231-13240.	2.3	36
103	Visible light activated photocatalytic behaviour of rare earth modified commercial TiO2. Materials Research Bulletin, 2014, 50, 183-190.	2.7	59
104	Influence of sol counter-ions on the visible light induced photocatalytic behaviour of TiO <sub>2</sub> nanoparticles. Catalysis Science and Technology, 2014, 4, 2134-2146.	2.1	26
105	Non-aqueous sol–gel synthesis through a low-temperature solvothermal process of anatase showing visible-light photocatalytic activity. RSC Advances, 2014, 4, 46762-46770.	1.7	18
106	Silver-Modified Nano-titania as an Antibacterial Agent and Photocatalyst. Journal of Physical Chemistry C, 2014, 118, 4751-4766.	1.5	81
107	A hydroxyapatite–Fe <sub>2</sub> O <sub>3</sub> based material of natural origin as an active sunscreen filter. Journal of Materials Chemistry B, 2014, 2, 5999-6009.	2.9	50
108	Fully quantitative X-ray characterisation of Evonik Aeroxide TiO2 P25®. Materials Letters, 2014, 122, 345-347.	1.3	66

#	Article	IF	CITATIONS
109	Molecular modeling of the piezoelectric effect in the ferroelectric polymer poly(vinylidene fluoride) (PVDF). Journal of Molecular Modeling, 2013, 19, 3591-3602.	0.8	78
110	Sol–gel synthesis, characterisation and photocatalytic activity of pure, W-, Ag- and W/Ag co-doped TiO2 nanopowders. Chemical Engineering Journal, 2013, 214, 364-375.	6.6	73
111	Modeling of switching and piezoelectric phenomena in polyvinylidenefluoride (PVDF). , 2013, , .		2
112	A Computational Study of the Properties and Surface Interactions of Hydroxyapatite. Ferroelectrics, 2013, 449, 94-101.	0.3	22
113	Natural Portuguese clayey materials and derived TiO2-containing composites used for decolouring methylene blue (MB) and orange II (OII) solutions. Applied Clay Science, 2013, 83-84, 91-98.	2.6	30
114	Introduction to the special issue for ISAF-ECAPD-PFM 2012. IEEE Transactions on Ultrasonics, Ferroelectrics, and Frequency Control, 2013, 60, 1549-1550.	1.7	0
115	Study of polar and electrical properties of Hydroxyapatite: Modeling and data analysis. , 2013, , .		0
116	Compositional and chromatic properties of strontium hexaferrite as pigment for ceramic bodies and alternative synthesis from wiredrawing sludge. Dyes and Pigments, 2013, 96, 659-664.	2.0	11
117	Nanosized titania modified with tungsten and silver: Microstructural characterisation of a multifunctional material. Applied Surface Science, 2013, 287, 276-281.	3.1	13
118	Phase composition, crystal structure and microstructure of silver and tungsten doped TiO2 nanopowders with tuneable photochromic behaviour. Acta Materialia, 2013, 61, 5571-5585.	3.8	53
119	Titanium dioxide modified with transition metals and rare earth elements: Phase composition, optical properties, and photocatalytic activity. Ceramics International, 2013, 39, 2619-2629.	2.3	47
120	Calcium phosphate-based materials of natural origin showing photocatalytic activity. Journal of Materials Chemistry A, 2013, 1, 6452.	5.2	57
121	Bacteria immobilisation on hydroxyapatite surface for heavy metals removal. Journal of Environmental Management, 2013, 121, 87-95.	3.8	77
122	Extraction and characterisation of apatite- and tricalcium phosphate-based materials from cod fish bones. Materials Science and Engineering C, 2013, 33, 103-110.	3.8	129
123	Aligned Co2Z Hexagonal Ferrite Fibers. Additional Conferences (Device Packaging HiTEC HiTEN &) Tj ETQq1 1 0.7	784314 rg 0.2	;BT_/Overlock
124	Polarization of poly(vinylidene fluoride) and poly(vinylidene fluoride-trifluoroethylene) thin films revealed by emission spectroscopy with computational simulation during phase transition. Journal of Applied Physics, 2012, 111, .	1.1	32
125	BioFerroelectricity: Diphenylalanine Peptide Nanotubes Computational Modeling and Ferroelectric Properties at the Nanoscale. Ferroelectrics, 2012, 440, 3-24.	0.3	47
126	Combinatorial Bulk Ceramic Magnetoelectric Composite Libraries of Strontium Hexaferrite and Barium Titanate. ACS Combinatorial Science, 2012, 14, 425-433.	3.8	23

#	Article	IF	CITATIONS
127	Chromatic Properties of Industrial Solid Waste Based Ferrites. Waste and Biomass Valorization, 2012, 3, 375-378.	1.8	4
128	Hexagonal ferrites: A review of the synthesis, properties and applications of hexaferrite ceramics. Progress in Materials Science, 2012, 57, 1191-1334.	16.0	1,981
129	Magnetic properties of randomly oriented BaM, SrM, Co2Y, Co2Z and Co2W hexagonal ferrite fibres. Journal of the European Ceramic Society, 2012, 32, 905-913.	2.8	57
130	The Rapid Discovery of Novel Dielectric and Magnetic Ceramics, and Structure-Property Relationships, through Combinatorial High Throughput Methods. Additional Conferences (Device Packaging HiTEC) Tj ETQq0 0 C	0 nggBT ∕Ov	e <b>d</b> lock 10 Tf
131	Local probing of magnetoelectric coupling in multiferroic composites of BaFe12O19–BaTiO3. Journal of Applied Physics, 2010, 108, .	1.1	43
132	Structures, phase transitions and microwave dielectric properties of the 6H perovskites Ba3BSb2O9, B=Mg, Ca, Sr, Ba. Journal of Solid State Chemistry, 2009, 182, 479-483.	1.4	12
133	Dielectric measurements on a novel Ba1 â~` x Ca x TiO3 (BCT) bulk ceramic combinatorial library. Journal of Electroceramics, 2009, 22, 245-251.	0.8	51
134	The Synthesis, Properties, and Applications of Columbite Niobates (M <sup>2+</sup> Nb <sub>2</sub> O <sub>6</sub> ): A Critical Review. Journal of the American Ceramic Society, 2009, 92, 563-577.	1.9	136
135	Dielectric loss caused by oxygen vacancies in titania ceramics. Journal of the European Ceramic Society, 2009, 29, 419-424.	2.8	155
136	Functional Ceramic Materials Database:  An Online Resource for Materials Research. Journal of Chemical Information and Modeling, 2008, 48, 449-455.	2.5	8
137	The effects of dielectric loss and tip resistance on resonator <i>Q</i> of the scanning evanescent microwave microscopy (SEMM) probe. Measurement Science and Technology, 2008, 19, 115502.	1.4	5
138	Bismuth-induced dielectric relaxation in the (1â^'x)La(Mg1â^•2Ti1â^•2)O3–xBi(Mg1â^•2Ti1â^•2)O3 perovskite sys Journal of Applied Physics, 2008, 104, .	stem. I.I	8
139	Broadband microwave-to-terahertz near-field imaging. IEEE MTT-S International Microwave Symposium Digest IEEE MTT-S International Microwave Symposium, 2007, , .	0.0	4
140	Dielectric relaxation and microwave loss in the La(Mg <sub>1/2</sub> Ti <sub>1/2</sub> )O <sub>3</sub> –(Na <sub>1/2</sub> Bi <sub>1/2</sub> )TiO <sub>3<!--<br-->perovskite ceramics. Journal of Materials Research, 2007, 22, 2676-2684.</sub>	sulz>	6
141	MgWO4, ZnWO4, NiWO4 and CoWO4 microwave dielectric ceramics. Journal of the European Ceramic Society, 2007, 27, 1059-1063.	2.8	205
142	Manufacture and measurement of combinatorial libraries of dielectric ceramics. Journal of the European Ceramic Society, 2007, 27, 3861-3865.	2.8	17
143	Manufacture and measurement of combinatorial libraries of dielectric ceramics. Journal of the European Ceramic Society, 2007, 27, 4437-4443.	2.8	35
144	Effect of sodium on the creep resistance of yttrium aluminium garnet (YAG) fibres. Journal of the European Ceramic Society, 2006, 26, 1577-1583.	2.8	18

#	Article	IF	CITATIONS
145	A mechanism for low-temperature sintering. Journal of the European Ceramic Society, 2006, 26, 2777-2783.	2.8	161
146	Low-temperature microwave and THz dielectric response in novel microwave ceramics. Journal of the European Ceramic Society, 2006, 26, 1845-1851.	2.8	22
147	Novel microwave dielectric LTCCs based uponV2O5 doped M2+Cu2Nb2O8 compounds (M2+=Zn, Co, Ni,) Tj ETQ	q1 1 0.78 2.8	4314 rgBT
148	The magnetic properties of aligned M hexa-ferrite fibres. Journal of Magnetism and Magnetic Materials, 2006, 300, 490-499.	1.0	45
149	V <sub>2</sub> O <sub>5</sub> -Doped M <sup>2+</sup> Cu <sub>2</sub> Nb <sub>2</sub> O <sub>8</sub> Compounds (M <sup>2+</sup> = Zn, Co, Ni, Mg & Ca) for Microwave Dielectric LTCCs. Materials Science Forum. 2006. 514-516. 264-268.	0.3	0
150	Evaluating the properties of dielectric materials for microwave integrated circuits. , 2006, , .		0
151	Characterization and Microwave Dielectric Properties of M2+Nb2O6 Ceramics. Journal of the American Ceramic Society, 2005, 88, 2466-2471.	1.9	153
152	The effects of sintering aids upon dielectric microwave properties of columbite niobates, M2+Nb2O6. Journal Physics D: Applied Physics, 2004, 37, 348-352. Effect of Sintering Aids upon Dielectric Microwave Properties of	1.3	28
153	ZnNb <sub>Ž</sub> O <sub>6</sub> , CoNb <sub>2</sub> O <sub>6</sub> , MgNb <sub>2</sub> O <sub>6</sub> and CaNb<:sub>:2<:/sub>:O<:sub>:6<:/sub> Columbite Niobates, Key Engineering Materials.	0.4	1
154	2004, 264-268, 1157-1160. Effect of Doping on the Dielectric Properties of Cerium Oxide in the Microwave and Farâ€Infrared Frequency Range. Journal of the American Ceramic Society, 2004, 87, 1233-1237.	1.9	116
155	Structure–Property Relations in <i>x</i> BaTiO <sub>3</sub> –(1â^' <i>x</i> )La(Mg <sub>1/2</sub> Ti <sub>1/2</sub> )O <sub>3</sub> Solid Solutions. Journal of the American Ceramic Society, 2004, 87, 584-590.	1.9	25
156	Sintering Behaviour of BaxSr1-xTiO3. Integrated Ferroelectrics, 2004, 62, 249-252.	0.3	7
157	Relationship between microwave and lattice vibration properties in Ba(Zn1/3Nb2/3)O3-based microwave dielectric ceramics. Journal Physics D: Applied Physics, 2004, 37, 1980-1986.	1.3	61
158	Temperature compensated niobate microwave ceramics with the columbite structure, M2+Nb2O6. Journal of the European Ceramic Society, 2003, 23, 2479-2483.	2.8	54
159	Structure and microwave dielectric properties of La(Mg0.5Ti0.5)O3–CaTiO3 system. Journal of the European Ceramic Society, 2003, 23, 2403-2408.	2.8	41
160	Microwave Dielectric Properties of Columbite-Structure Niobate Ceramics, M <sup>2+</sup> Nb <sub>2</sub> O <sub>6</sub> . Key Engineering Materials, 2002, 224-226, 1-4.	0.4	31
161	Crystallisation of hexagonal M ferrites from a stoichiometric sol–gel precursor, without formation of the α-BaFe2O4 intermediate phase. Materials Letters, 2002, 57, 537-542.	1.3	67

A halide free route to the manufacture of microstructurally improved M ferrite (BaFe12O19 and) Tj ETQq0 0 0 rgBT\_ $\frac{10}{2.8}$  Verlock  $\frac{10}{42}$  Tf 50 6

#	Article	IF	CITATIONS
163	Decomposition, shrinkage and evolution with temperature of aligned hexagonal ferrite fibres. Acta Materialia, 2001, 49, 4241-4250.	3.8	35
164	The manufacture of partially-stabilised and fully-stabilised zirconia fibres blow spun from an alkoxide derived aqueous sol–gel precursor. Journal of the European Ceramic Society, 2001, 21, 19-27.	2.8	26
165	Title is missing!. Journal of Materials Science, 2001, 36, 4805-4812.	1.7	45
166	The synthesis and characterization of the hexagonal Z ferrite, Sr3Co2Fe24O41, from a sol-gel precursor. Materials Research Bulletin, 2001, 36, 1531-1538.	2.7	43
167	Magnetic properties of nanocrystalline CoFe2O4 powders prepared at room temperature: variation with crystallite size. Journal of Magnetism and Magnetic Materials, 2001, 232, 71-83.	1.0	307
168	Halide removal from BaM (BaFe12O19) and SrM (SrFe12O19) ferrite fibers via a steaming process. Journal of Materials Research, 2001, 16, 3162-3169.	1.2	13
169	A method for the preparation of aligned fibre samples for magnetic measurement using VSM. Journal of Magnetism and Magnetic Materials, 2000, 218, 1-4.	1.0	7
170	The sintering behaviour, mechanical properties and creep resistance of aligned polycrystalline yttrium aluminium garnet (YAG) fibres, produced from an aqueous sol–Gel precursor. Journal of the European Ceramic Society, 1999, 19, 1747-1758.	2.8	52
171	Polycrystalline yttrium aluminium garnet (YAG) fibres produced from the steaming of an aqueous sol–gel precursor. Materials Letters, 1999, 39, 173-178.	1.3	14
172	Blow spun strontium zirconate fibres produced from a sol-gel precursor. Journal of Materials Science, 1998, 33, 3229-3232.	1.7	20
173	The Microwave Properties of Aligned Hexagonal Ferrite Fibers. Journal of Materials Science Letters, 1998, 17, 973-975.	0.5	31
174	Title is missing!. Journal of Materials Science, 1998, 33, 5229-5235.	1.7	11
175	The manufacture of yttrium aluminium garnet (YAG) fibres by blow spinning from a sol-gel precursor. Journal of the European Ceramic Society, 1998, 18, 1759-1764.	2.8	41
176	The manufacture and characterisation of aligned fibres of the ferroxplana ferrites Co2Z, 0.67% CaO-doped Co2Z, Co2Y and Co2W. Journal of Magnetism and Magnetic Materials, 1998, 186, 313-325.	1.0	67
177	The manufacture, characterisation and microwave properties of aligned M ferrite fibres. Journal of Magnetism and Magnetic Materials, 1998, 186, 326-332.	1.0	76
178	Aligned hexagonal ferrite fibres of Co2W, BaCo2Fe16O27 produced from an aqueous sol–gel process. Journal of Materials Science, 1997, 32, 873-877.	1.7	29
179	Magnetic Co2Y ferrite, Ba2Co2Fe12O22 fibres produced by a blow spun process. Journal of Materials Science, 1997, 32, 365-368.	1.7	25
180	Hexagonal Ferrite Fibres and Nanofibres. Solid State Phenomena, 0, 241, 1-68.	0.3	10

#	Article	IF	CITATIONS
181	Cork-derived hierarchically porous hydroxyapatite with different stoichiometries for biomedical and environmental applications. Materials Chemistry Frontiers, 0, , .	3.2	9
182	Extraction and characterisation of cellulose nanocrystals from pineapple peel. International Journal of Food Studies, 0, , 24-33.	0.5	24
183	Effective decolouration of cationic dyes by silica gel prepared from Tunisian sands and TiO2/silica gel composites: dual adsorption and photocatalytic processes. , 0, 179, 368-377.		1